

Spin-dependent elastic scattering of electrons from a ferromagnetic glass, $\text{Ni}_{40}\text{Fe}_{40}\text{B}_{20}$

D. T. Pierce, R. J. Celotta, and J. Unguris
National Bureau of Standards, Washington, D. C. 20234

H. C. Siegmann
Swiss Federal Institute of Technology, 8093 Zurich, Switzerland
(Received 5 April 1982)

The dependence of the elastic scattering of electrons on the relative direction of the spin of the incident electron with respect to the magnetization of the ferromagnetic glass $\text{Ni}_{40}\text{Fe}_{40}\text{B}_{20}$ was measured at various energies, angles, and temperatures. We show that this scattering is liquidlike, i.e., effects of crystal diffraction are negligible. Also, multiple scattering of electrons contributes less than 30% to the intensity in the backward scattering direction. Under these conditions, and with correction for electron attenuation, the scattering is atomlike. This yields a first insight into the spin dependence of electron scattering from single magnetic atoms in a metallic environment. The surface magnetization was found to decrease with temperature with the same power law as the bulk magnetization at low temperature in agreement with theoretical predictions by Mills and Maradudin.

I. INTRODUCTION

Following measurements of the spin dependence in elastic scattering from a single-crystal Ni(110) surface,¹ scattering of slow spin-polarized electrons from magnetic surfaces has emerged recently as one of the most promising ways to study surface magnetism.¹⁻⁴ In recent measurements on a ferromagnetic glass, $\text{Ni}_{40}\text{Fe}_{40}\text{B}_{20}$, it was also shown that both the intensity of inelastic scattering from the sample, as well as the intensity of the current absorbed by the sample depend on the spin polarization of the incident beam relative to the sample magnetization.⁵ In this paper we present a more complete description of this extension of spin-polarized electron scattering to amorphous materials and present new results on the elastic scattering of polarized electrons from $\text{Ni}_{40}\text{Fe}_{40}\text{B}_{20}$.

In contrast to the scattering from the surface of a single crystal where diffraction produces well-collimated beams which have strong variations with energy and angle, the scattering from a noncrystalline metallic glass is diffuse. It is the purpose of this paper to show that within reasonable approximations our observations on $\text{Ni}_{40}\text{Fe}_{40}\text{B}_{20}$ should be accounted for by the spin-dependent scattering from single surface atoms corrected for attenuation, which is due mainly to plasmon and electron-hole-pair creation. This simplicity arises from the absence of effects of diffraction in a glass and from the relative weakness of multiple scattering in the backward scattering direction as will be shown

below.

Different theoretical methods have been used to treat the spin dependence in electron scattering from magnetic surfaces. Some investigations treated the magnetic scattering in the first Born approximation.^{6,7} Dynamical polarized low-energy diffraction (PLEED) calculations have been carried out for Ni(110) by Wang,⁸ and a series of calculations over several years on different Fe surfaces have been described by Feder.³ However, it is still an open question as to what model should be used to account for the effects of exchange and correlation in the scattering of electrons from single magnetic atoms. Only with the correct atomic scattering factors can one proceed to crystalline materials and determine surface magnetic structures and other surface magnetic data of high current interest. The measured energy and angle dependence of the spin-dependent scattering asymmetry which we report in this paper represents a first step in this direction.

II. EXPERIMENTAL CONSIDERATIONS

We used a ferromagnetic glass as a target and measured the elastic backscattering of electrons with incident-electron spin parallel or antiparallel to the target magnetization. The metallic glass $\text{Ni}_{40}\text{Fe}_{40}\text{B}_{20}$ is well suited for these experiments because it is easily magnetized to saturation, and it is sufficiently disordered to neglect effects of crystal diffraction. A thin strip of the sample, $16 \times 2 \times 0.03 \text{ mm}^3$, was saturated by the remanent

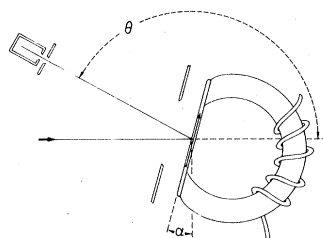


FIG. 1. Schematic of the scattering geometry. Sample closes the magnetic circuit of the small electromagnet. Sample and electromagnet can be rotated about an axis perpendicular to the figure to change the angle of incidence α . Scattering angle θ is determined by the position of the Faraday cup relative to the incident-electron-beam direction.

magnetization of a C-shaped iron electromagnet as pictured in Fig. 1. The magnetization was reversed by applying a current pulse to the coil.

A beam of spin-polarized electrons from a GaAs photocathode⁹ was incident on the sample at an angle α to the surface normal. The intensity I_{\uparrow} or I_{\downarrow} of electrons scattered elastically into a movable Faraday cup was measured for the spin polarization respectively parallel and antiparallel to the majority-spin direction in the sample (respectively antiparallel and parallel to the magnetization). We measured the normalized asymmetry in the spin-dependent elastic scattering which is defined as

$$S = (1/|P_0 \cos \alpha|)(I_{\uparrow} - I_{\downarrow}) / (I_{\uparrow} + I_{\downarrow}), \quad (1)$$

where the factor $1/|P_0 \cos \alpha|$ corrects for the fact that at an angle of incidence α , only the component of the polarization of the incident beam that is collinear with the magnetization of the sample contributes to S . The spin-averaged scattered intensity $I = (I_{\uparrow} + I_{\downarrow})/2$ is measured simultaneously. Measurements of S and I were made as a function of energy, scattering angle θ , and azimuth ϕ . The Faraday-cup aperture was enlarged to increase the signal from the weak diffusely scattered intensity; the full cone angle defined by the aperture and the intersection of the beam with the sample was 9° . (The solid angle subtended by the aperture was 0.019 sr.)

The glass was cleaned by 500-eV Ar^+ -ion bombardment at an angle of incidence of 54° . In this series of experiments, the sample was not annealed after ion bombardment. The surface contamination was monitored by Auger spectroscopy using a cylindrical mirror analyzer. Ion bombardment at room temperature removed oxygen and sulfur contamination but left a residue of carbon. The amount of C on the surface was comparable to the

amount of B. Sputtering at liquid-nitrogen temperature produced surfaces with approximately half as much C. Carbon was found on the surface, even though the bulk carbon composition was less than 0.06 wt. %. The Ni-to-Fe peak ratio remained nearly constant with sputtering as expected from previous work¹⁰ which showed that Ni and Fe have similar sputtering cross sections. There was some variation of up to 25% in the absolute value of the scattering asymmetry S for the same scattering conditions which might be attributable to slight changes in the sample surface composition, sputter damage, etc. The nature of such variations was to scale S without changing the shape of the curves as a function of energy or angle.

The effect of stray magnetic fields which can deflect the electron beam or change the apparent scattering angle was also investigated. The $\text{Ni}_{40}\text{Fe}_{40}\text{B}_{20}$ sample, which closes the magnetic circuit of the electromagnet, has a very high susceptibility leading to low stray fields. It is apparent from Fig. 1 that for symmetry reasons stray magnetic fields near the center of the sample must be predominantly parallel or antiparallel to the magnetization. We found that the field along the magnetization axis, taken as the x direction, decreased as a function of distance z from the surface as $B_x = B_0 e^{-z/d}$ where $d \approx 0.5$ cm. To magnetize the sample, the electromagnet was energized with a current chosen such that the remanent magnetization of the electromagnet core would be ample to maintain the sample in saturation when the electromagnet current was reduced to zero. The spatial variation of the stray field, which came mostly from the electromagnet core, was measured; B_0 was found to be 0.6 G for the conditions used in the scattering studies reported here. Calculations of electron trajectories as a function of electron energy were made for this stray-field distribution. The stray field was calculated to cause a shift of the beam on the sample surface of Δy and a change in angle from nominal normal incidence of $\Delta \gamma$. As seen in the inset of Fig. 2, it is a change in a plane perpendicular to the plane of Fig. 1. The variation of Δy and $\Delta \gamma$ with energy from 20 to 400 eV is shown in Fig. 2. Calculations of this type have been verified¹¹ by measuring the shift in position of the electron beam at the Faraday cup, $2\Delta y$, for the case of a well-collimated beam diffracted from an Fe crystal for conditions where $B_0 = 4$ G. Note that Δy and $\Delta \gamma$ are linear in B_0 . Considering the solid angle accepted by the Faraday cup, the changes in position and the changes in the actual scattering angle from the nominal angle are quite small.

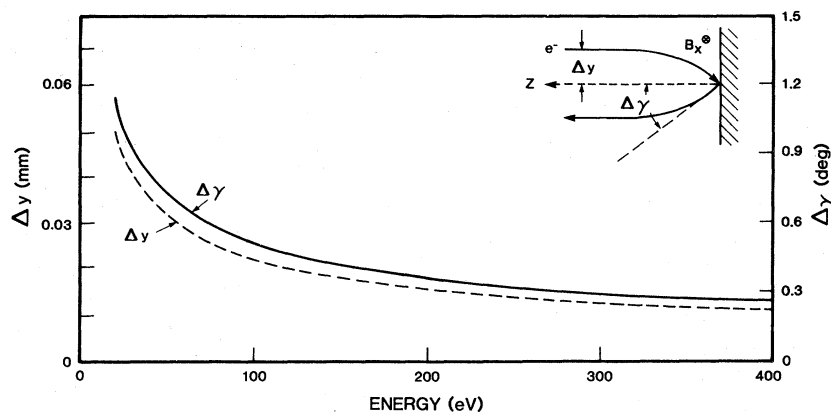


FIG. 2. Stray-magnetic-field-induced displacements Δy and changes of angle $\Delta\gamma$ of an electron beam incident on the sample shown as a function of energy. Δy and $\Delta\gamma$ are defined in the insert. Stray-field distribution giving these curves is described in the text.

Elastic scattering could be observed down to electron energies of 2 eV in the backward direction ($\theta=166^\circ$). For electron energies below 25 eV, the kinetic energy of the electrons leaving the gun was kept constant at 25 eV, and the incident-electron energy was varied by applying a retarding voltage to the sample. Retarding energy analyzer potential plots¹² shows that electrons maintain most of their energy until quite near the sample surface thereby causing the effect of the stray field to be less than expected from an extrapolation of Fig. 2. Changes in angle of incidence due to the retarding field for 7-eV electrons have been found to be less than 2° for $\alpha \leq 30^\circ$ in low-energy polarized-electron scattering measurements of a W(100) surface.¹³

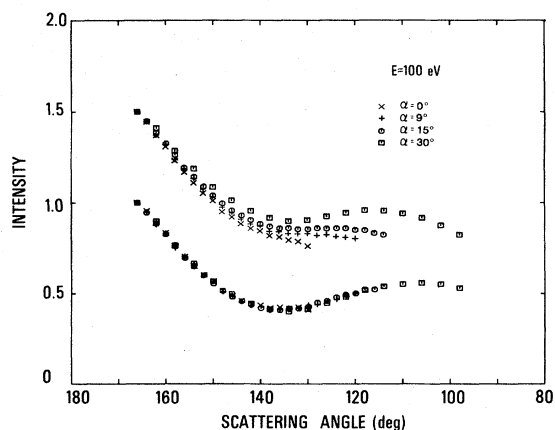


FIG. 3. Elastically scattered intensity shown as a function of scattering angle for a primary energy of 100 eV and angles of incidence of 0° , 9° , 15° , and 30° . Curves are normalized at $\theta=166^\circ$ and displaced upwards from the lower curve where the curves have been corrected for electron attenuation.

III. SPIN-AVERAGED ELASTIC SCATTERING INTENSITY

Schilling and Webb¹⁴ compared low-energy-electron scattering from liquid Hg to gaseous Hg, thereby providing some way to estimate the relative contributions of multiple scattering of the electrons and of attenuation of the electrons by inelastic processes. They found for the case of backscattering that the angular and energy dependence of the scattering is very similar to that of the free atom. In the following, we show that the scattering behavior of the metallic glass is similar to liquid Hg.

The θ dependence of the elastic scattering intensity is shown in Fig. 3. The experimental curves normalized at polar scattering angle $\theta=166^\circ$ are shown displaced upward. The shape of the measured curves depends on the angle of incidence α . However, when correction is made for the different attenuation of the electrons at different angles of incidence as done for liquid Hg,¹⁴ the measurements for different α exactly coincide as seen in the lower set of curves. The fact that the scattering curves are independent of α shows that crystal structure and the orientation of the sample surface can be neglected in scattering from $\text{Ni}_{40}\text{Fe}_{40}\text{B}_{20}$.

As discussed by Lagally and Webb¹⁵ and Schilling and Webb,¹⁴ when the scattered intensity is independent of crystal structure and orientation, the variation in intensity is representative of the atomic scattering cross section $|f(e,\theta)|^2$ except for the contribution of multiple scattering. Since higher-order scattering is expected to have a relatively flat angular dependence,¹⁴ the depth of the minima in the scattered intensity allows an estimate to be

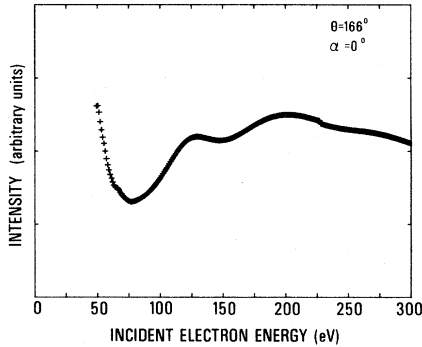


FIG. 4. Elastically backscattered intensity shown as a function of energy for a beam at normal incidence which is scattered 166° .

made of the contributions of multiple scattering. If it is assumed that apart from the multiple scattering the intensity at the minimum is zero, the intensity at the minimum provides an upper limit on the contribution of multiple scattering. For example, the intensity at the relative minimum at $\theta=135^\circ$ in the experimental curve of Fig. 3 is about one-third that of the backscattered intensity at $\theta=166^\circ$. We estimate therefore that the multiple-scattering contribution at $\theta=166^\circ$ is less than one-third of the total scattering at this angle.

The dependence of the scattered intensity on the incident-electron energy is shown in Fig. 4 for a scattering angle $\theta=166^\circ$ at normal incidence, $\alpha=0^\circ$. The measurements range from 50 to 300 eV. The intensity minimum at 75 eV is also found in calculations¹⁶ for electron scattering from atomic Ni and Fe.

IV. SPIN DEPENDENCE OF THE ELASTIC SCATTERING INTENSITY

The spin-dependent asymmetry S in the scattered intensity, defined in Eq. (1), can be caused by two spin-dependent interactions: (1) an interaction which arises from the net ordered spin density in the sample, and (2) a spin-orbit interaction which is proportional to $\vec{s} \cdot \vec{L}$ and arises from the interaction of the spin \vec{s} of the incident electron with its own orbital angular momentum \vec{L} about the scattering center. The spin-orbit interaction is large in heavy atoms such as W where it has been studied in detail.¹⁷⁻¹⁹ In low- Z metals like Ni and Fe the effect is small; we measured S in $\text{Ni}_{40}\text{Fe}_{40}\text{B}_{20}$ due to the spin-orbit interaction to be $<0.1\%$ for $75 < E < 100$ eV and increasing to 0.5% at 175 eV for a scattering angle $\theta=150^\circ$. In the case of a Ni single crys-

tal, where S can be enhanced by interference effects in the diffraction, values of S due to the spin-orbit interaction as high as 10% have been observed.²⁰

For our studies of magnetic scattering from $\text{Ni}_{40}\text{Fe}_{40}\text{B}_{20}$, the contributions to S due to the spin-orbit interaction were kept small by having the polarization of the incident beam lie in the scattering plane and by minimizing the stray magnetic field outside the sample. As seen in Fig. 2, the stray field can cause the electron to have motion in a plane perpendicular to the nominal scattering plane. The incident polarization is perpendicular to this scattering plane giving rise to a spin-orbit contribution which cannot be separated out by reversing the magnetic field. However, it is possible to check for the presence of such a spin-orbit contribution by measuring S as a function of increasing applied field once the sample is saturated. The spin-orbit interaction due to motion in the increasing stray field would cause S to increase whereas S due to the exchange interaction remains constant. As seen from the hysteresis curve shown in Fig. 5, no such increase in S in the region of saturation was observed thereby establishing that stray-field-induced spin-orbit contributions are not important here. The sharp switching of the sample magnetization observed in the hysteresis curves is typical for ferromagnetic glasses. The magnetic scattering measurements were made for both directions of the sample magnetization in order to account for any apparatus asymmetry.

The variation in S as a function of scattering angle due to magnetic interactions is shown in Fig. 6 for a 90-eV beam incident on the sample at $\alpha=30^\circ$. The spin dependence is largest at large scattering angles and decreases to a minimum before rising slightly again. The measurement of S in the inset of Fig. 6 at fixed incident energy and scattering angle shows that it is independent of angle of in-

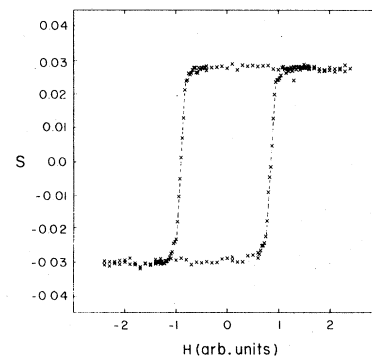


FIG. 5. Hysteresis curve $S(H)$ for electron energy $E=100$ eV and scattering angle $\theta=166^\circ$.

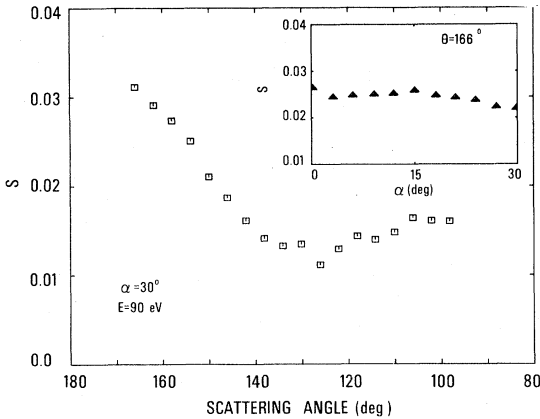


FIG. 6. Spin-dependent asymmetry S of the elastic scattering as a function of scattering angle for a 90-eV beam with 30° angle of incidence. Inset shows the insensitivity of S to angle of incidence when other parameters remain fixed.

cidence from 0° to 30° . It is not necessary to correct (as was done in Fig. 3) specifically for attenuation, to the extent that it is independent of spin,²¹ since the same factors occur in both the numerator and denominator of S .

Again, we see that the scattering depends only on the scattering angle and is independent of the orientation of the surface. Also, in contrast to the spin-orbit interaction which is positive, negative or zero depending on the orientation of the incident-spin and the scattering plane, the magnetic scattering is independent of the azimuthal orientation of the scattering plane and was found to depend only on the relative orientation of the incident-electron spin and the spins in the surface. The essentially atomic nature of this scattering should make it possible to directly test the theoretical models. Our results, such as the increase in S with increasing scattering angle, provide a test for theories of the mechanism of magnetic scattering.

Further information which should lead to a better understanding of the scattering is contained in measurements of S over a wide energy range. For the energy dependence measurements, we chose the maximum scattering angle accessible in apparatus, $\theta=166^\circ$, because there the relative contribution of multiple scattering is a minimum as discussed in the analysis of Fig. 3. In Fig. 7 we show S as a function of incident-electron energy from 2 to 300 eV ($\theta=166^\circ, \alpha=0$). Measurements from 300 to 500 eV showed that S remains small and does not change sign. Although S is always below 3% in the curve of Fig. 7, there is a considerable structure including changes of sign at 12 and 50 eV. For in-

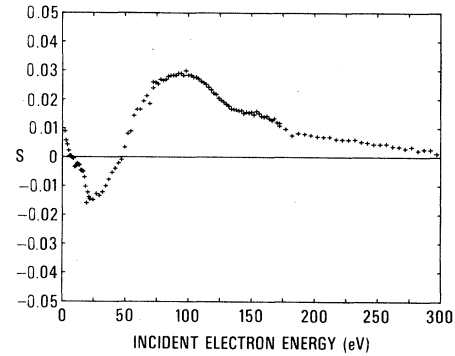


FIG. 7. Spin dependence S of the elastic scattering as a function of the energy with a beam at normal incidence and scattering through an angle of 166° .

cident energies less than 12 eV and greater than 50 eV, S is positive, meaning that incident-electron spins that are parallel to the majority-spin direction scatter more strongly than those that are anti-parallel.

Some success has been achieved in calculating the shape of the curve in Fig. 7 assuming single-atom scattering and using spin-dependent exchange potentials.²² A simple model has been proposed²³ which attributes the spin dependence in scattering from ferromagnets to a spin-dependent imaginary part of the potential, that is to a spin-dependent electron attenuation length. However, such a model alone does not explain the variations and sign changes measured in Fig. 7.

V. SPIN DEPENDENCE OF THE ABSORBED CURRENT

Siegmann *et al.*⁵ showed recently the current absorbed in a magnetic sample depends on the orienta-

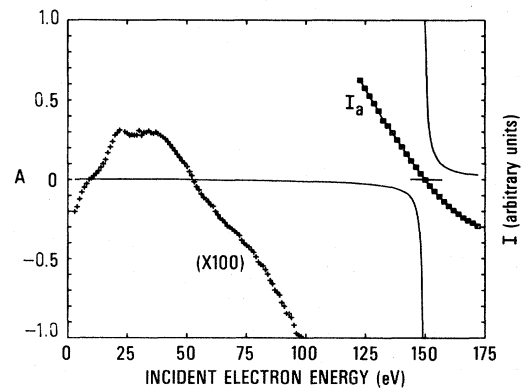


FIG. 8. Spin dependence of the absorbed current as a function of energy is given by the solid line and below 100 eV magnified 100 times by the plus. Spin-averaged current absorbed I_a is shown by \square near the energy where the secondary yield is unity.

tion of the spin polarization of the incident-electron beam. The absorbed current is equal to the number of incident electrons reaching the sample minus the number of elastically and inelastically backscattered electrons and true secondaries leaving the sample. From an analysis of the inelastic scattering, it was concluded that it is predominantly the spin dependence of the elastic scattering which gives rise to the spin dependence of the absorbed current.

The curve of the spin dependence of the absorbed current from this earlier work⁵ is reproduced here as Fig. 8 because a striking comparison can be made to Fig. 7. The normalized spin-dependent asymmetry A of the absorbed current is defined analogously to S ,

$$A = (1/|P_0 \cos \alpha|)(i_{\uparrow} - i_{\downarrow})/(i_{\uparrow} + i_{\downarrow}), \quad (2)$$

where i_{\uparrow} and i_{\downarrow} are the absorbed currents for the polarization of the incident beam respectively parallel and antiparallel to the majority-spin direction in the surface. Figure 8 shows the variation of A as a function of the energy of the primary electrons. Below 100 eV, A is less than 1%, but structure in A is still easily measured.

Below 9 eV, A is negative and it becomes negative again at 50 eV. Note that this behavior is just the opposite of S in Fig. 7 and that the zero crossings are very nearly the same. At very low energies where more parallel than antiparallel spins are elastically scattered (Fig. 7), the absorbed current induced by antiparallel spins is greater than that for parallel spins. This implies that the spin dependence of the elastic scattering is the cause of the spin dependence of the absorbed current.

At higher energy, A diverges as seen in Fig. 8. At the energy E_0 the spin-averaged absorbed current $I_a = (i_{\uparrow} + i_{\downarrow})/2$ is zero; that is, the number of electrons incident on the sample is exactly balanced by those leaving, and the secondary yield is unity. The spin dependence of the absorbed current relative to the spin-independent current is greatly enhanced near E_0 . Siegmann *et al.*⁵ noted that this provides the basis for a new type of spin detector. This "absorbed current spin analyzer" which can also be based²⁴⁻²⁶ on the spin-orbit interaction has an efficiency superior²⁷ to the best Mott detectors.

VI. TEMPERATURE DEPENDENCE OF THE SURFACE MAGNETIZATION

At temperatures $T \neq 0$, magnons are excited in a ferromagnet, causing a decrease of the saturation magnetization and adding a magnetic term in the

specific heat. At low temperatures, the ratio of the magnetization $M_b(T)$ of the bulk to the bulk magnetization at zero temperature $M_b(0)$ decreases as

$$M_b(T)/M_b(0) = 1 - B_b T^{3/2} + \dots, \quad (3)$$

as first shown by Bloch. The constant B is characteristic of the low-temperature long-wavelength spin waves or magnons. The next higher-order term proportional to $T^{5/2}$ has been found²⁸ to be small for amorphous ferromagnets at temperatures less than half the Curie temperature, T_c .

Mills and Maradudin²⁹⁻³¹ predicted that the surface magnetization $M_s(T)$ decreases twice as fast, but still according to $T^{3/2}$ in the low-temperature regime. Although this result was obtained within the Heisenberg model, it should also hold for itinerant systems at low temperatures where the magnons have long wavelengths.^{32,33} Differences between itinerant and localized systems should become prominent only in the short-wavelength regime of the spin waves. It has been a challenge for experimentalists to test the predictions of Mills and Maradudin. Observation of the surface term in the specific heat should reveal the presence of surface magnons, but these experiments have proven to be very difficult and so far inconclusive.³²

Measurement of the asymmetry S in the spin-dependent elastic scattering of polarized electrons is another means to test for the effects of surface magnons. One obtains a measure of the average surface magnetization M_s^* representing the average magnetization in a sheet of thickness corresponding to the probing depth of the electrons. For example, electrons which scatter in Ni at an energy of 90 eV have a mean free path for inelastic scattering of $\lambda = 5$ Å.³⁴ Thus, in our experiments we expect the electrons to have a probing depth of approximately 2.5 Å corresponding to travel, on the average, of $\lambda/2$ into and out of the sample.

The deviation of the surface magnetization from that of the bulk due to surface magnons decreases with distance into the bulk. It is important to compare the depth of the surface disturbance with the probing depth of the electrons to determine to what extent the measurement of S is influenced by the bulk magnetization. From the dispersion relation for thermal magnons, $Dq^2 = k_B T$, Mills and Maradudin introduce a characteristic length which is the reciprocal of the magnon wave vector,

$$q^{-1} = (D/k_B)^{1/2}. \quad (4)$$

Typical values³⁵ of D for such ferromagnetic glasses are $D \simeq 100$ meV Å² which for $T = 100$ K gives

$q^{-1}=3.4 \text{ \AA}$ or about two atomic layers. However, the actual decay of the surface disturbance as computed from the expression given by Mills and Maradudin [Eq. (5.16)] of Ref. 29 or Eq. (IV.23) of Ref. 32] is rapid; even for $q^{-1}\simeq 2$ layers the surface disturbance is confined to the first layer and is reduced to about 20% of the first-layer value at the second layer. Since the average electron probing depth is about 1.5 layers, we estimate that roughly half of the scattering is from the first layer. Thus, although the measured S does not result solely from the surface magnetization it is sufficiently surface sensitive to detect deviations from the bulk behavior.

Since the surface magnetization is the quantity to be measured, it is necessary to ask how S is related to $M_s^*(T)$. Although S is frequently nearly proportional to M_s^* this need not be true in general.³⁶ We know from symmetry that S must be proportional to an odd power of M_s^* , i.e.,

$$S = \alpha M_s^* + \beta M_s^{*3} + \gamma M_s^{*5} + \dots \quad (5)$$

In a single crystal where electrons are diffracted and multiply scattered, it is not clear which term is dominant in a diffraction spot, but it can be argued³⁶ that $S \simeq M_s^*$ as $T \rightarrow T_c$. Hence magnetic single crystals are ideal for tests of the high-temperature regime where short-wavelength magnons prevail. When there is only single scattering, we have $S = \alpha M_s^*$ at all temperatures. For the case of $\text{Ni}_{40}\text{Fe}_{40}\text{B}_{20}$ there is no diffraction and the multiple scattering is weak in the backscattering direction where we measure the temperature dependence of S so that to a good approximation $S = \alpha M_s^*$. Magnetic glasses are ideal for tests of the effects of long-wavelength surface magnons by spin-polarized

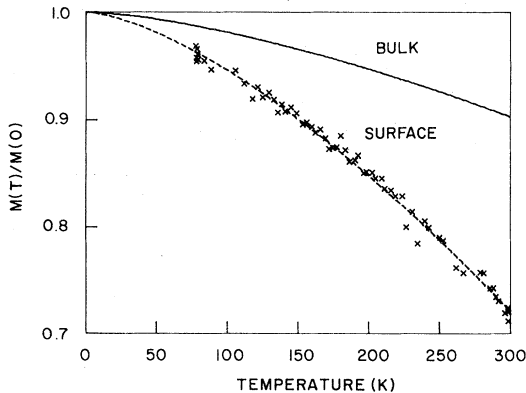


FIG. 9. Variation with temperature of the surface magnetization (points) measured by polarized-electron scattering is compared to that of the bulk (solid line) determined by conventional methods.

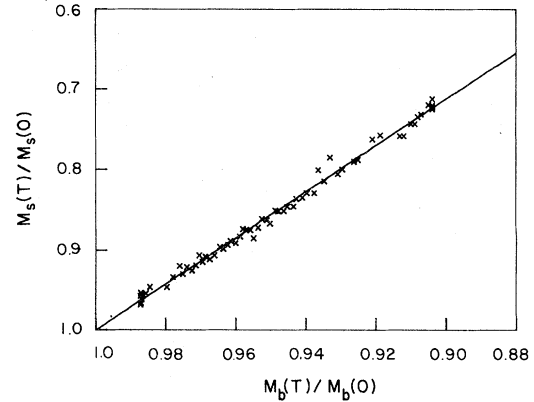


FIG. 10. $M_s^*(T)/M_s^*(0)$ and $M_b(T)/M_b(0)$ have a linear relationship indicating that they vary with temperature according to the same power law. Temperature range is from 0 to 300 K which is about $0.4T_c$.

electron scattering.

The temperature dependence of the relative magnetization $M(T)/M(0)$ in $\text{Ni}_{40}\text{Fe}_{40}\text{B}_{20}$ is shown in Fig. 9. $M_b(T)$ was measured³⁷ with a moving sample magnetometer from 4 to 280 K. The data were fit well by Eq. (3) with $M_b(0)=0.96$ bohr magnetons/atom of alloy and $B_b \simeq 19 \times 10^{-6} \text{ deg}^{-3/2}$. The temperature dependence of the surface magnetization $M_s^*(T)/M_s^*(0)$ was obtained by measuring S for elastic scattering of electrons at a scattering angle $\theta=166^\circ$ and at an energy $E=90 \text{ eV}$ where λ is close to a minimum and $S(E)$ close to a maximum. The data points in Fig. 9 correspond to $(S^+ - S^-)/2$ where S^+ and S^- are obtained with a positive and negative magnetization direction, respectively. This removes residual asymmetries in the scattering introduced by the apparatus.

To test the prediction of Mills and Maradudin that the surface and bulk magnetization decrease with temperature according to the same power law, we plotted the measured S vs M_b . A straight line was obtained showing that M_s^* is directly proportional to M_b and hence both obey the same temperature power law. This result is illustrated in Fig. 10 where we plot $M_s^*(T)/M_s^*(0)$ vs $M_b(T)/M_b(0)$ for one of the experimental runs. The points fall in a straight line over the whole temperature range up to $T \simeq 0.4T_c$. The Curie temperature of $\text{Ni}_{40}\text{Fe}_{40}\text{B}_{20}$ is not known with certainty, but is in the neighborhood of 700 K where the glass crystallizes. There is an uncertainty in $M_s^*(0)$ due to the lack of data at low temperature; note, however, that a change in $M_s^*(0)$ only changes the slope of the line in Fig. 10 and does not change our conclusion about the power-law behavior.

The other prediction of Mills and Maradudin was that the surface magnetization decrease twice as fast as the bulk, i.e., $B_s = 2B_b$. The line in Fig. 10 is least-squares linear fit to the points and the slope of the line is B_s/B_b . If the $T^{3/2}$ behavior observed for $M_s^*(T)$ from 80 to 300 K is assumed in the extrapolation to obtain $M_s^*(0)$ as was done in Figs. 9 and 10, one finds that B_s is about 3 times B_b . This is actually a lower limit since some of the bulk behavior is also being probed which would tend to reduce the measured B_s . Thus we find that the surface magnetization decreases more rapidly than was predicted.²⁹

VII. CONCLUSION

Ferromagnetic glasses are especially well suited to obtain insight into magnetic scattering at surfaces. The scattering is independent of surface orientation, not complicated by crystalline diffraction effects, and is dominated by the effective atomic scattering factors. This permits measurements which are closely related to the energy and angle dependence of the atomic scattering factors. The energy and angle variations of the spin dependence provide a means of testing different models of spin-dependent

interactions. With the spin-dependent atomic scattering factors determined, one can proceed to crystalline materials and determine magnetic structures and other surface magnetic data of current interest for many basic and applied questions. Measurement of the temperature dependence of the surface magnetization, M_s^* for $T \ll T_c$, shows that $M_s^* \propto M_b$ in the regime of the long-wavelength magnons. This was predicted by Mills and Maradudin in 1967, and is here confirmed for the first time.

ACKNOWLEDGMENTS

We are greatly indebted to H. J. Guntherodt for providing the sample of $\text{Ni}_{40}\text{Fe}_{40}\text{B}_{20}$ ferromagnetic glass. We are grateful to F. Hulliger for the measurements of the bulk magnetization and A. Galejs for calculating electron trajectories in stray magnetic fields. We wish to thank S. W. Wang for many stimulating discussions and for communicating her calculations to us prior to publication. We also want to thank D. L. Mills for helpful discussions concerning the temperature dependence of the surface magnetization. This work was supported in part by the Office of Naval Research.

-
- ¹R. J. Celotta, D. T. Pierce, G.-C. Wang, S. D. Bader, and G. P. Felcher, *Phys. Rev. Lett.* **43**, 728 (1979).
²D. T. Pierce and R. J. Celotta, *Adv. Electron. Electron Phys.* **56**, 219 (1981).
³R. Feder, *J. Phys. C* **14**, 2049 (1981).
⁴S. F. Alvarado, M. Campagna, and H. Hopster, *Phys. Rev. Lett.* **48**, 51 (1982).
⁵H. C. Siegmann, D. T. Pierce, and R. J. Celotta, *Phys. Rev. Lett.* **46**, 452 (1981).
⁶L. A. Vredevoe and R. E. De Wames, *Phys. Rev.* **176**, 684 (1968).
⁷X. I. Saldaña and J. Helman, *Phys. Rev. B* **16**, 4978 (1977).
⁸S. W. Wang, *Solid State Commun.* **36**, 847 (1980).
⁹D. T. Pierce, R. J. Celotta, G.-C. Wang, W. N. Unertl, A. Galejs, C. E. Kuyatt, and S. R. Mielczarek, *Rev. Sci. Instrum.* **51**, 478 (1980).
¹⁰T. J. Chuang and K. Wandelt, *Surf. Sci.* **81**, 355 (1979).
¹¹J. Unguris, D. T. Pierce, and R. J. Celotta (unpublished).
¹²T. H. DiStefano and D. T. Pierce, *Rev. Sci. Instrum.* **41**, 180 (1970).
¹³E. G. McRae, D. T. Pierce, G.-C. Wang, and R. J. Celotta, *Phys. Rev. B* **24**, 4230 (1981).
¹⁴J. S. Schilling and M. B. Webb, *Phys. Rev. B* **2**, 1665 (1970).
¹⁵M. G. Lagally and M. B. Webb, *Phys. Rev. Lett.* **21**, 1388 (1968).
¹⁶M. Fink, M. R. Martin, and G. A. Somorjai, *Surf. Sci.* **29**, 303 (1972).
¹⁷M. Kalisvaart, M. R. O'Neill, T. W. Riddle, F. B. Dunning, and G. K. Walters, *Phys. Rev. B* **17**, 1570 (1978).
¹⁸G.-C. Wang, R. J. Celotta, and D. T. Pierce, *Phys. Rev. B* **23**, 1761 (1981).
¹⁹R. Feder and J. Kirschner, *Surf. Sci.* **103**, 75 (1981).
²⁰S. F. Alvarado, H. Hopster, R. Feder, and H. Pleyer, *Solid State Commun.* **39**, 1319 (1981).
²¹The spin dependence of the attenuation is expected to be quite small. R. W. Rendell and D. R. Penn, *Phys. Rev. Lett.* **45**, 2057 (1980).
²²S. W. Wang (unpublished).
²³R. Feder, *Solid State Commun.* **31**, 821 (1979).
²⁴M. Erbudak and N. Müller, *Appl. Phys. Lett.* **38**, 575 (1981).
²⁵R. J. Celotta, D. T. Pierce, H. C. Siegmann, and J. Unguris, *Appl. Phys. Lett.* **38**, 577 (1981).
²⁶D. T. Pierce, S. M. Girvin, J. Unguris, and R. J. Celotta, *Rev. Sci. Instrum.* **52**, 1437 (1981).
²⁷M. Erdubak and G. Ravano, *J. Appl. Phys.* **52**, 5032 (1981).
²⁸S. N. Kaul, *Phys. Rev. B* **24**, 6550 (1981).
²⁹D. L. Mills and A. A. Maradudin, *J. Phys. Chem. Solids* **28**, 1855 (1967).

- ³⁰D. L. Mills, *Comments Solid State Phys.* **4**, 28 (1971).
- ³¹D. L. Mills, *Comments Solid State Phys.* **4**, 95 (1972).
- ³²D. L. Mills, in *Surface Excitations*, edited by V. M. Agramovich and R. Loudon (North-Holland, Amsterdam, 1982).
- ³³J. Mathon, *Phys. Rev. B* **24**, 6588 (1981).
- ³⁴J. E. Demuth, P. M. Marcus, and D. W. Jepsen, *Phys. Rev. B* **11**, 1460 (1975).
- ³⁵F. E. Luborsky, in *Ferromagnetic Materials*, edited by E. P. Wohlfarth (North-Holland, Amsterdam, 1980), Vol. 1, p. 451.
- ³⁶R. Feder and H. Pleyer, *Surf. Sci.* (in press), have considered this question in more detail.
- ³⁷F. Hulliger (private communication).